

## Estimation of the Population of Neutrophils Induced to Differentiate from the MPRO Mouse Promyelocytic Cell Line

Fransiskus X. Ivan, Roy E. Welsch, Vincent T.K. Chow, and Jagath C. Rajapakse

**Abstract**— Neutrophils derived from induced-differentiated mouse promyelocyte (MPRO) cell lines provide an alternative source of mouse neutrophils for *in vitro* experiments, substituting for primary mouse neutrophils that are normally obtained by sacrificing mice. One issue with using induced-differentiated MPRO cells (or NEUTs) is that they are usually composed of not only mature neutrophils, but also neutrophil precursors. Here, we report on an assessment of an automated image analysis system to estimate mature neutrophil proportion in giemsa-stained NEUTs, and compare the accuracy with manual cell counting and flow cytometry results.

### INTRODUCTION

Mouse promyelocyte (MPRO) cell lines are a GM-CSF dependent neutrophil cell line derived from genetically engineered bone marrow cells inserted with a truncated RARalpha403 gene (ATCC CRL-11422). MPRO cells can be induced to differentiate into neutrophils by supplementing with all-trans retinoic acid (ATRA) [1]. The states of differentiating MPRO cells include the defined stages of neutrophil maturation, i.e. promyelocyte, myelocyte, metamyelocyte, band cell, and mature (segmented) neutrophil. These stages are defined according to the morphology of the nucleus and the composition of granules (primary, secondary and specific granules). Promyelocyte and myelocyte have spherical nuclei, but their granule compositions are different. Promyelocyte mainly contains primary granules and in myelocyte, secondary granules appear. Metamyelocyte elicit the early stage of nucleus segmentation, where the nucleus is indented, forming a broad-bean-like shape. In the next stage, the nucleus transforms to a band shape, hence it is called a band cell. Specific granules start to appear during this stage. Finally,

the mature neutrophil can be recognized from its multi-lobed (2-5 lobes) nucleus and more specific granules are formed. Under giemsa staining, the cytoplasm of promyelocyte is dark blue-purple, and at the later stages, the cytoplasm becomes transparent.

Induced-differentiated MPRO cell lines (NEUTs) have been shown to be a potential source of neutrophils for experiments. Neutrophils in NEUTs show similar responses to normal neutrophils, that include chemotaxis, respiratory burst, and phagocytosis [2]. Recently we observed that neutrophils from NEUTs release neutrophil extracellular traps (NETs), i.e. extracellular DNA fibers armed with granule and nuclear components that can kill microorganisms [3]. Hence, these demonstrate the potential of full functionalities of neutrophils in NEUTs to substitute for the use of mouse neutrophils that are traditionally isolated from blood drawn by sacrificing the mice. However, a problem with using NEUTs is that the population of NEUTs contains not only neutrophils, but also neutrophil precursors. Thus, NEUTs need to be routinely checked for neutrophil proportion before executing an experiment.

Two approaches are available to estimate the proportion of mature neutrophils: cell counting of giemsa-stained NEUTs and flow cytometry. The giemsa-staining approach is much cheaper than flow cytometry since it does not require antibodies as a marker, but merely a drop of dye solution. Furthermore, giemsa-stained NEUTs can be prepared in 10 minutes, while the antibody staining procedure for flow cytometry requires at least 30 minutes. However, thousands of cells can be inspected within seconds by a flow machine, while only a few hundreds of giemsa-stained cells are reasonably inspected within 10 minutes by an experienced laboratory scientist. Thus, flow cytometry is much more accurate in estimating mature neutrophil proportions compared to manual cell counting.

Here, we propose an automated image analysis system as an alternative to laborious manual cell counting to estimate mature neutrophil proportions in giemsa-stained NEUTs. Some sophisticated automated systems are available to classify giemsa-stained blood cells; however, their performance is shown to be dependent on the source of the blood samples [4]. In addition, the systems were specifically developed to analyze a smear of human blood sample. Hence, different algorithms and training data sets are required to deal with cytospin giemsa-stained NEUTs, which are cells of mouse origin and contain different mixtures of cells.

Manuscript received April 15, 2011. This work was supported in whole or in part by the Singapore-MIT Alliance and Singapore-MIT Alliance for Research and Technology.

F. X. Ivan is with Computation and Systems Biology, Singapore-MIT Alliance, Nanyang Technological University, Singapore 637460. E-mail: fran0021@ntu.edu.sg.

R. E. Welsch is with Sloan School of Management, Massachusetts Institute of Technology, Cambridge, Massachusetts 02142, USA and Computation and Systems Biology, Singapore-MIT Alliance, Nanyang Technological University, Singapore 637460. E-mail: rwelsch@mit.edu.

V. T. K. Chow is with Department of Microbiology, Yong Loo Lin School of Medicine, National University of Singapore, Singapore 117597. E-mail: vincent\_chow@nuhs.edu.sg.

J. C. Rajapakse is with Bioinformatics Research Centre, Nanyang Technological University, Singapore 637553 and Computation and Systems Biology, Singapore-MIT Alliance, Nanyang Technological University, Singapore 637460. E-mail: asjagath@ntu.edu.sg.

## I. MATERIALS AND METHODS

**MPRO Cell Cultures and Differentiation.** MPRO cells were cultured at 37°C (5% CO<sub>2</sub> in air atmosphere) in Isocove's modified Dulbecco's medium (IMDM) containing 4 mM L-glutamine, 1.5 g/L sodium bicarbonate, 10 ng/mL murine GM-CSF, and 20% heat inactivated fetal bovine serum (FBS). To induce the differentiation of MPRO cells into neutrophils, 10 μM of all-trans retinoic acid (ATRA) was supplemented into the complete growth medium (following the results from [1]). Differentiated cell lines (viability > 90% based on trypan blue exclusion) were collected within 5 days after supplementing ATRA.

**Flow Cytometry.** Differentiated MPRO cells were washed with phosphate-buffer saline (PBS) before and after incubation with or without anti-mouse PerCP-Cy<sup>TM</sup>5.5 rat anti-mouse Ly-6G (BD Pharmingen, San Diego, CA) for 20 minutes at 4°C. Flow cytometry was performed with a Cytomics FC500 Series Flow Cytometry System (Beckman Coulter) to identify the percentage of neutrophils (Ly-6G positive cells) and the data were analyzed by using WinMDI ver 2.9 (Bio-Soft NET, <http://en.bio-soft.net>).

**Giemsa-staining and Imaging.** Fifty micro-liter samples containing  $2.5\text{-}5.0 \times 10^4$  of either MPRO cells (day 0) or differentiated MPRO cells (1-5 days after adding the ATRA), were prepared onto slides by performing May-Grünwald-Giemsa-stained cytopspin. Brightfield images of cytopspinned cells were taken by using a MIRAX MIDI slide scanner (Carl Zeiss, Germany). Cell images at 40× magnification were then sampled from the scanned area.

**Cell, nucleus and cytoplasm segmentation.** We employed an iterative method to segment the cells. For each iteration, color images were converted into gray scale images and contrast-limited adaptive histogram equalization [5] was used to improve contrast in the images. A global image threshold using Otsu's method [6] was then applied to identify objects (cell regions); small objects were not considered and holes in each object were filled. Next, minimum bounding boxes associated with each object were determined and used to obtain color images of each object. A threshold of image size was determined to identify images containing a single cell. Images were pre-processed in the next iteration if their size was bigger than the threshold; and if no significant reduction was found for the identified objects, the images were not considered. Four level Otsu's segmentation was applied to images of a single cell to determine nucleus and cytoplasm regions.

**Feature Extraction and Selection.** Sixty one morphological features of detected nucleus regions, which include 30 Zernike moments described in [7] and shape measurements such as area, perimeter, and solidity, were derived. In addition, seven statistics for pixel value measurement of gray scale segmented nucleus and cytoplasm regions were included. Feature selection was performed by using a

minimal-redundancy-maximal-relevance (mRMR) criterion [8].

**Classifying Images of a Single Cell.** Two classes of images of a single cell were defined, one represents the (mature) neutrophil and the other represents the non-neutrophil (other type of cells). A *k*-nearest neighbor classifier, combined with mRMR feature selection, was trained to classify cell images. For this, we manually selected 1000 images of a single cell that could reasonably be classified as neutrophils and non-neutrophils (500 images for each class) and derived the morphological features of their nucleus and pixel measurement as described previously.

## II. RESULTS

### A. Cell stages observed in NEUTs are highly diverse.

Unlike peripheral blood which consists of more or less discrete stages of cell population (red blood cells, mature neutrophils, etc.), NEUTs consist of maturing neutrophil cells of varying stages. The stages observed in NEUTs often do not clearly belong to the defined stages of neutrophil differentiation (promyelocyte to mature neutrophil), but also in between of those defined stages. In addition to this, mitotic stages of promyelocyte and myelocyte could also possibly be observed in NEUTs. Furthermore, although the events are rarely observed, MPRO cells may also differentiate into eosinophils. To illustrate the diversity of NEUTs, snapshots of giemsa-stained NEUTs collected on day 1 and day 3 after ATRA stimulation are shown in Fig. 1.

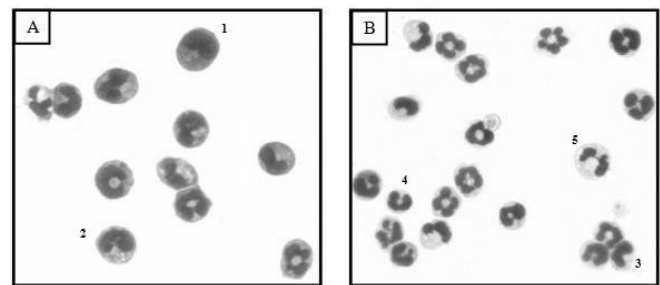


**Fig. 1.** The diversity of induced-differentiated MPRO population on day one (A) and day three (B) after supplementing ATRA. Best representatives of defined stages of neutrophil differentiation are marked with the numbers: 1-promyelocyte, 2-myelocyte, 3-metamyelocyte, 4-band cell, and 5-mature neutrophil.

### B. Iterative global image thresholding may isolate a single cell from cell clusters.

Cell clusters are often observed in cytopspinned MPROs or NEUTs. Thus, a segmentation technique is required to single out the cells for further inspection by an automated image analysis system. We demonstrated that a simple iterative global image thresholding combined with contrast-limited adaptive histogram equalization (described in Materials and Methods) may isolate single cells from the clusters. The

algorithm is able to split a bigger cluster into smaller clusters or eventually single cells. An illustration of a result given by the method is given in Fig. 2. For further processing, images containing cell debris or more than one cell could be removed by specifying a threshold for the size of the cells.

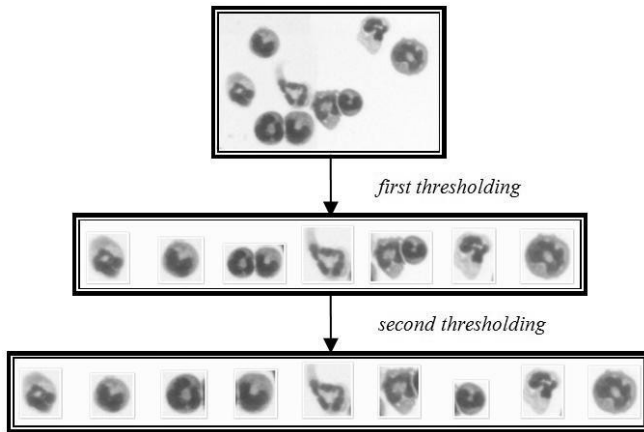


Fig. 2. An example of cell segmentation results output by the iterative global image thresholding (two iterations).

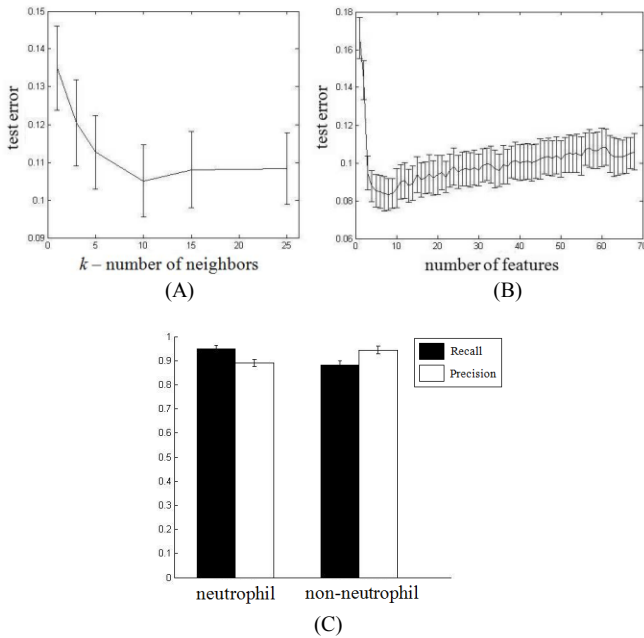


Fig. 3. (A) Test error of  $k$ -NN for various  $k$ , the number of neighbors (all features were used for the classification). (B) Test error of  $k$ -NN ( $k=10$ ) using the first  $k$  features selected by mRMR criterion. (C) Recall and precision of each class given by  $k$ -NN ( $k=10$ ) based on mRMR's first five features. Error bars in (A), (B) and (C) were based on 100 experiments.

### C. Training the $k$ -nearest neighbor ( $k$ -NN classifier) and selecting features to classify cell images.

We manually selected 1000 images of a single cell, 500 for the (mature) neutrophil class and 500 for the non-neutrophil class for training the  $k$ -nearest neighbors. From each class, 40% of images from each class (neutrophil and non-neutrophil) were randomly selected as training data and the

rest were used as test data for each experiment. To select the best  $k$  for  $k$ -NN, all features were used to classify the cell image. As suggested by Fig. 3A, which shows the test error of  $k$ -NN over varying value of  $k$ , we chose  $k=10$  for further experiments.

Next, feature selection by the mRMR criterion was performed and it helped to improve the performance of the  $k$ -NN classifier. As shown in Fig. 3B, using the first eight features gave the highest performance, where the mean test error was about 0.083. This was significantly lower than the mean test error given by  $k$ -NN that used all features for classification, which is about 0.105. The first eight features ordered by mRMR were ratio between perimeter and area, location of the centroid, the average intensity of cytoplasm region, Zernike moment 2-0, Zernike moment 4-0, solidity, area, and Zernike moment 6-4 (seven features are based on nucleus regions, except the third feature). Fig. 3C shows the recall and precision of  $k$ -NN based on selected features. It can be seen that the recall is higher than the precision for neutrophil class, but the opposite holds for the non-neutrophil class.

### D. Neutrophil proportion can be estimated accurately by the proposed automated system.

The proposed automated system invoked the iterative cell segmentation and 10-NN classifier based on the first eight mRMR features and the 1000 manually selected images of a single cell for prediction. For the purpose of testing the automated system to estimate neutrophil proportion in NEUTs, six populations of NEUTs of different cultures were collected for flow cytometry and two sets of cytopinned giemsa staining. Ten fields of circular cytopspin area (two each from the center, top-right, bottom-right, bottom-left, and top-left) were sampled at 40 $\times$  magnification and input to the automated system. Blinded manual cell counting was also performed to estimate neutrophil proportion from each cytopinned NEUTs.

Table 1. Comparison of manual and automated neutrophil estimation

Culture	Repeat	Neutrophil proportion (number of events/cells)		
		Flow cytometry	Automated	Manual
1	1	12.7% (20,000)	18.7% (852)	24.8% (230)
	2		19.1% (637)	31.0% (216)
2	1	11.3% (20,000)	8.5% (442)	25.6% (215)
	2		12.4% (781)	13.4% (268)
3	1	10.7% (20,000)	13.1% (1191)	22.3% (310)
	2		9.4% (685)	17.8% (292)
4	1	9.5% (20,000)	7.5% (521)	20.6% (180)
	2		5.6% (631)	8.8% (216)
5	1	8.5% (20,000)	7.6% (620)	12.7% (220)
	2		8.6% (680)	12.3% (204)
6	1	15.7% (20,000)	14.9% (748)	12.2% (295)
	2		17.9% (733)	20.6% (155)

Table 1 tabulates the estimated neutrophil proportion given by flow cytometry, the automated system, and manual cell counting. The results suggest that flow cytometry and the

automated system gave a comparable estimate for most of the cultures, while the manual cell counting tends to overestimate neutrophil proportion and gives a higher variance over the repeats.

### III. DISCUSSION

As a neutrophil source, the MPRO cell line provides vast opportunities in neutrophil research, which include the study on the interaction between neutrophils and microorganisms and the formation and release of neutrophil extracellular traps. Biologists may avoid the technical and ethical difficulties of isolating neutrophils from mice. From our experience in inducing MPRO differentiation, a population of NEUTs containing more than 50% neutrophils is obtainable, as confirmed by flow cytometry. However, the neutrophil yields over the same or various treatments and timing for harvesting were often below 50%. Thus, a technique that consistently gives a high neutrophil proportion from induced-differentiation of MPRO cells needs to be developed. For this purpose, the development of an automated image analysis system to estimate the neutrophil proportion from giemsa-stained NEUTs may play a part in reducing the cost or difficulty of future research.

In this report, we demonstrated that an accurate estimate of neutrophil proportion in NEUTs can be obtained by using an automated system that incorporates relatively simple techniques of image analysis, machine learning and statistical sampling. Despite the 8.3% probable misclassification, the neutrophil proportion in giemsa-stained NEUTs estimated by the proposed automated system is often comparable to that given by flow cytometry. The automated system was shown to perform better than manual techniques, which frequently overestimated the neutrophil proportion. The overestimations were likely due to the preference for counting regions that contain both neutrophil and non-neutrophil, which is an example of a bias that can occur during manual cell counting. Furthermore, a higher variance of manually estimated neutrophil proportions could be expected as fewer cells were being counted.

Next, MPRO cell lines are not only useful as an alternative neutrophil source, but it can also be used to study neutrophil maturation. The genomic and proteomic analysis of the myeloid differentiation program using MPRO cell lines have been reported [9]. Some further study that could be carried out using MPROs is to associate protein expressions with the stages of the neutrophil maturation. A fluorescence imaging technique is required in this case and perhaps, an automated classification of fluorescence-labeled nuclei and cell images may help to infer an association in a high-throughput fashion. However, based on our experience, classifying images of giemsa-stained differentiating MPRO cells into three or more classes is quite challenging (test error went up to 30%). A typical problem with this task, similar to the case highlighted in [10], is the misclassification of a cell to its closest class neighbor. Hence, a new approach needs to be

developed and assessed to deal with classification of three or more cell classes.

### IV. CONCLUSION

Automated classification of the images of neutrophils and non-neutrophils in giemsa-stained NEUTs can be performed accurately. This allowed the development of a cheap and less laborious automated image analysis system to estimate neutrophil proportion. An extension of this work is to develop a system that can classify differentiating MPRO cells into three or more classes (e.g. promyelocyte, myelocyte, metamyelocyte, band cell, and mature neutrophil).

### ACKNOWLEDGMENTS

The technical assistances of Dr. Dahai Zheng (Singapore-MIT Alliance for Research and Technology) for imaging and Poh Wee Peng, Thong Khar Tiang, Nalini Srinivasan, and Chan Yue Ng (Yong Loo Lin School of Medicine, National University of Singapore) for flow cytometry are gratefully acknowledged.

### REFERENCES

- [1] B. S. Johnson, R. A. Chandraratna, R. A. Heyman, E. A. Allegretto, L. Mueller, S. J. Collins, "Retinoid X receptor (RXR) agonist-induced activation of dominant-negative RXR-retinoic acid receptor alpha403 heterodimers is developmentally regulated during myeloid differentiation," *Mol. Cell. Biol.*, vol. 19, no. 5, pp.3372–3382, May 1999.
- [2] P. Gaines, J. Chi, N. Berliner, "Heterogeneity of functional responses in differentiated myeloid cell lines reveals EPRO cells as a valid model of murine neutrophil functional activation," *J. Leukoc. Biol.*, vol.77, no. 5, pp.669–679, May 2005.
- [3] V. Brinkmann, U. Reichard, C. Goosmann, B. Fauler, Y. Uhlemann, D. S. Weiss, Y. Weinrauch, A. Zychlinsky, "Neutrophil extracellular traps kill bacteria," *Science*, vol. 303, no. 5663, pp.1532–1535, Mar 2004.
- [4] H. Ceelie, R. B. Dinkelaar, W. van Gelder, "Examination of peripheral blood films using automated microscopy; evaluation of Diffmaster Octavia and Cellavision DM96," *J. Clin. Pathol.*, vol. 60, no. 1, pp.72–79, Jan. 2007.
- [5] K. Zuiderveld, "Contrast limited adaptive histogram equalization," *Graphic Gems IV*, San Diego: Academic Press Professional, 1994, pp.474–485.
- [6] N. Otsu, "A threshold selection method from gray-level histograms," *IEEE Trans. Systems, Man, and Cybernetics*, vol. 9, no. 1, pp.62–66, 1979.
- [7] M. V. Boland, M. K. Markey, and R. F. Murphy, "Automated recognition of patterns characteristics of subcellular structures in fluorescence microscopy images," *Cytometry*, vol. 33, no. 3, pp. 366–375, Nov.1998.
- [8] H. Peng, F. Long, and C. Ding, "Feature selection based on mutual information: criteria of max-dependency, max-relevance, and min-redundancy," *IEEE Trans. Pattern Anal. Mach. Intell.*, vol. 27, no. 8, pp. 1226–1238, Aug. 2005.
- [9] Z. Lian, Y. Kluger, D. S. Greenbaum, D. Tuck, M. Gerstein, N. Berliner, S. M. Weissman, P. E. Newburger, "Genomic and proteomic analysis of the myeloid differentiation program: global analysis of gene expression during induced differentiation in the MPRO cell line," *Blood*, vol. 100, no. 9, pp.3209–3220, Nov. 2002.
- [10] M. Bins, L. H. van Montfort, T. Timmers, G. H. Landeweerd, E. S. Gelsema, and M. R. Halie, "Classification of immature and mature cells of the neutrophil series using morphometrical parameters," *Cytometry*, vol. 3, no. 6, pp. 435–438, Jan. 1983.